Special issue: the best papers of SBTA 2025

# Hygrothermal behavior of façade with thermal mortar in Porto Alegre and Lisbon

## *Desempenho higrotérmico de fachada com argamassa térmica em Porto Alegre e em Lisboa*


## Abstract

This study evaluated the hygrothermal performance of façades coated with thermal mortar containing expanded cork aggregates. The façades were exposed to the climatic conditions of Porto Alegre (Brazil) and Lisbon (Portugal). Thermal mortars have lower thermal conductivity than conventional ones. This property offers potential for improved thermal comfort, enhanced energy efficiency, and greater sustainability when produced with bio-based materials such as cork. Numerical simulations with WUFI Pro 7.1 quantified heat and moisture transport in a double ceramic wall with an unventilated air layer. Results showed higher moisture contents in Lisbon. The north façade in Lisbon performed similarly to the south façade of Porto Alegre, mainly due to wind-driven rain. No risks of mold growth were identified on the interior surface. External condensation was assessed by hours at 100% relative humidity on exterior surfaces. The south façades recorded more hours, three to four times more frequent in Lisbon. Monthly thermal transmittance coefficients met local standards except in some summer months. Thermal mortars were viable under these conditions. Further optimization is recommended by considering water absorption of finishes, temperature- and moisture-dependent thermal conductivity and vapor permeability, real interior conditions, and ventilation within the air layer.


**Keywords:** Hygrothermal behavior. Water content. Local hygrothermal loads. External condensation. Thermal transmittance. Thermal mortar. Insulation.


[1]***Jéssica Deise Bersch**
[1]Universidade de Lisboa
Lisboa - Portugal
jessica.d.bersch@tecnico.ulisboa.pt

[2]**Angela Borges Masuero**
[2]Universidade Federal do Rio Grande do Sul
Porto Alegre - RS - Brasil
angela.masuero@ufrgs.br

[3]**Denise Dal Molin**
[3] Universidade Federal do Rio Grande do Sul
Porto Alegre - RS - Brasil
dmolin@ufrgs.br

[4]**Inês Flores-Colen**
[4]Universidade de Lisboa
Lisboa - Portugal
ines.flores.colen@tecnico.ulisboa.pt



**Recebido em 31/08/25**
**Revisado em 12/10/25**
**Aceito em 13/11/25**


*autor correspondente


## Resumo

*Este estudo avaliou o comportamento higrotérmico de fachadas revestidas com argamassa térmica contendo agregados de cortiça expandida, submetidas às condições climáticas de Porto Alegre (Brasil) e Lisboa (Portugal). Argamassas térmicas apresentam condutibilidade inferior às convencionais, oferecendo potencial para conforto térmico, eficiência energética e maior sustentabilidade quando produzidas com materiais biológicos, como a cortiça. Simulações numéricas com o software WUFI Pro 7.1 quantificaram transporte de calor e umidade em uma parede cerâmica dupla com camada de ar não ventilada. Os resultados indicaram teores de umidade mais elevados em Lisboa, com a fachada norte apresentando desempenho similar à sul de Porto Alegre, principalmente devido à chuva dirigida. Não foram identificados riscos de desenvolvimento de fungos na superfície interna. O potencial de condensação externa, avaliado pelo número de horas com umidade relativa de 100% na superfície externa, foi maior nas fachadas sul, com intensidade três a quatro vezes superior em Lisboa. Os coeficientes mensais de transmitância térmica atenderam às normas locais, exceto em alguns meses de verão. As argamassas térmicas mostraram-se viáveis, mas recomenda-se otimização do estudo considerando absorção de água dos acabamentos, condutibilidade térmica e permeabilidade ao vapor dependentes da temperatura e umidade, condições interiores reais, e ventilação na camada de ar.*


***Palavras-chave:*** *Desempenho higrotérmico. Teor de umidade. Carga higrotérmica. Condensação externa. Transmissão térmica. Argamassa térmica. Isolamento.*



BERSCH, J. D.; MASUERO, A. B.; DAL MOLIN, D. C.; FLORES-COLEN, I. Hygrothermal behavior of façade with thermal mortar in Porto Alegre and Lisbon. **Ambiente Construído**, Porto Alegre, v. 26, e149938, jan./dez. 2026.
ISSN 1678-8621 Associação Nacional de Tecnologia do Ambiente Construído.
http://dx.doi.org/10.1590/s1678-86212026000100951

# 1 Introduction

Controlling heat transfer in building components is crucial for achieving optimal energy and thermal performance (FIBP, 2019). Although investments in efficiency are increasing, most funds originate from a few European countries, making it more challenging to achieve low-carbon, efficient, and resilient buildings worldwide (UNEP, 2021), especially given the global prevalence of energy poverty (Che; Zhu; Wang, 2021). The current building stock is also crucial for sustainability, as it requires renovations that reduce greenhouse gas emissions and address energy concerns (European Commission, 2020).

In this context, improving façade thermal performance can involve multilayer insulation systems with thermal mortars. These materials are suitable for both new and, especially, existing buildings, as they adapt to cracks and irregular surfaces, common in older structures. Additionally, they offer adjustable thickness, are easy to apply, and do not require anchoring points (Posani; Veiga; Freitas, 2023; Parracha *et al.*, 2024a). This contrasts with External Thermal Insulation Composite System (ETICS) which use rigid insulating panels. With thermal conductivities below 0.2 W/(m·K) at 10 °C (ECS, 2010), thermal mortars slow heat transfer, helping to improve indoor thermal comfort (Pengfei; Chi; Wang, 2021).

Nevertheless, although thermal insulation benefits buildings, solutions with low thermal inertia, such as ETICS, can increase façade surface moisture through external condensation, leading to soiling and biological growth (Künzel, 2007; Flood; Scott; Gleeson, 2016). Furthermore, thermal inertia influences heat fluxes in building envelopes, and its effect on energy efficiency depends on the thermal transmittance coefficients used (Rodrigues *et al.*, 2019). Both these fluxes and coefficients change over time as they respond to climatic conditions (Flood; Scott; Gleeson, 2016). Additionally, moisture in insulation layers raises thermal conductivity, thereby reducing thermal performance (Malanho; Veiga; Farinha, 2021).

The use of thermal mortars is expected to grow (Parracha *et al.*, 2024a). In a March 2025 Scopus search for "thermal mortar" in titles, abstracts, and keywords, 40 studies were identified; 27 were published since 2020. Figure 1, generated using VOSviewer v1.6.18 (for bibliometric networks) with a minimum of five co-occurrences, illustrates the main keywords and their interconnections.

Figure 1 highlights an initial focus on the mechanical characteristics, thermal performance, and composition of thermal mortars. More recent studies examine how these materials age. In hygrothermal performance studies, Posani, Veiga and Freitas (2022) emphasize the importance of analyzing coating systems with all their layers, finding that separately assessed thermal mortar specimens exhibit water absorption coefficients up to 75% higher than those tested within the full multilayer insulation systems. Building on this, Pedroso *et al.* (2023) demonstrate good moisture control for thermal mortars with aerogel, reporting that the final finishing layers greatly affect performance. Furthermore, Pinchard *et al.* (2024) report a 30% increase in thermal conductivity for thermal mortars with cork aggregates after artificial aging equivalent to 10 years in Lisbon's natural conditions.

Figure 1 – **Keyword network visualization for articles including the term "thermal mortar"**

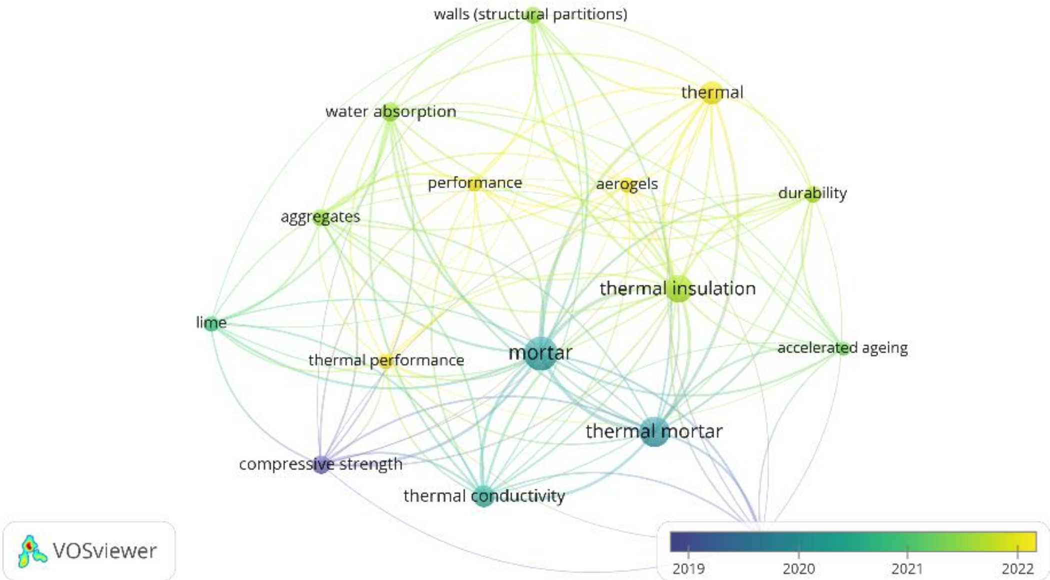

The hygrothermal behavior of façades, referring to the interaction of heat and moisture within exterior wall assemblies, can be evaluated through numerical simulations. WUFI Pro is a software program designed for dynamic modeling of heat and mass transfer, enabling the investigation of how they are distributed within walls under different climate conditions (Evrard *et al.*, 2014). In this case, liquid transfer coefficients, which indicate how easily moisture moves through walls, are calculated based on Künzel's exponential law (Fino; Tadeu; Simões, 2018). Relative humidity is used as the driving potential in both the sorption and capillary regions. This simplifies the transport process to a pure diffusive model, which relies on Fick's diffusion law, describing how substances move from areas of high concentration to areas of low concentration (Künzel, 1995; Fang; Chen; Wu, 2020; Guizzardi, 2014).

In this context, since the combination of heat and moisture transport significantly impacts building physics, occupants' health and comfort, and energy efficiency (Verma *et al.*, 2022), this article analyzes the hygrothermal performance of a façade externally coated with a multilayer insulation system containing a thermal mortar with cork aggregates. Expanded cork aggregates were selected due to their promising thermal properties, including low thermal conductivity coefficients, and because they constitute a by-product of industrial cork production (Borges; Flores-Colen; Brito, 2018; Brás; Leal; Faria, 2013), aligning with sustainability objectives.

The cities of Porto Alegre (latitude: 30° 01′ 58.8″ S; longitude: 51° 13′ 48.0″ W (UNGEGN, 2025)) in Brazil and Lisbon (latitude: 38° 43′ 33.6″ N; longitude: 9° 7′ 31.9″ W (UNGEGN, 2025)) in Portugal were selected for the numerical simulations. Both north- and south-facing orientations were considered. Porto Alegre has a Köppen-Geiger climate classification of Cfa, indicating a temperate climate with no dry season and hot summers (Beck *et al.*, 2018). This is commonly referred to as a humid subtropical climate (Liu *et al.*, 2022). Lisbon, by contrast, is classified as Csa, characterized by dry summers (Beck *et al.*, 2018). This corresponds to a Mediterranean climate with hot summers (Liu *et al.*, 2022). In both cities, the use of coating mortars is usual (Gaspar; Brito, 2005; Kleber, 2018), especially for existing buildings (Almeida *et al.*, 2023; INE; LNEC, 2013).

The analysis focused on moisture contents, total hygrothermal loads, potential for external surface condensation, and thermal transmittance. The goal was to understand the behavior of the façade system with an external thermal mortar coating under different climatic conditions. The cities were intentionally selected since they present differences but are not completely divergent. They correspond to locations where mortars, at least the conventional ones, are effectively used. Thus, the sensitivity of the insulation to the exposure conditions could be discussed.

This study investigates the effect of multilayer thermal mortars incorporating cork aggregates on façade performance, focusing on their ability to control moisture, condensation, and regulate heat transfer. By combining experiments and simulations in Porto Alegre and Lisbon, the study demonstrates the real-world impact of climate on insulation, providing actionable insights for sustainable, energy-efficient building design. Furthermore, the research opens doors to innovation by outlining several opportunities for future studies.

# 2 Experimental program

Figure 2 summarizes the methodology defined for the experimental program, as detailed in the Materials and Methods sections. The coating mortars were experimentally characterized, primarily in terms of their hygrothermal properties. On the other hand, the characterization of ceramic bricks was not the primary focus of this paper; therefore, their properties were selected from the WUFI Pro 7.1 database (FIBP, 2019), based on a typical brick chosen for the investigated locations and systems. With the complete assembly, numerical modelling of the façades was carried out, considering both north and south orientations, to identify water contents, hygrothermal loads, and the risk of external condensation, and to provide an initial attempt at characterizing transient thermal transmission.

Within the limitations of the study, three main simplifications were adopted to streamline the model:

(a) the dependency of thermal conductivity and water vapor permeability from moisture content was not included;

(b) the air cavity was assumed non-ventilated; and

(c) standardized indoor climate conditions were assumed.

Figure 2 - **Methodology used in the experimental program**

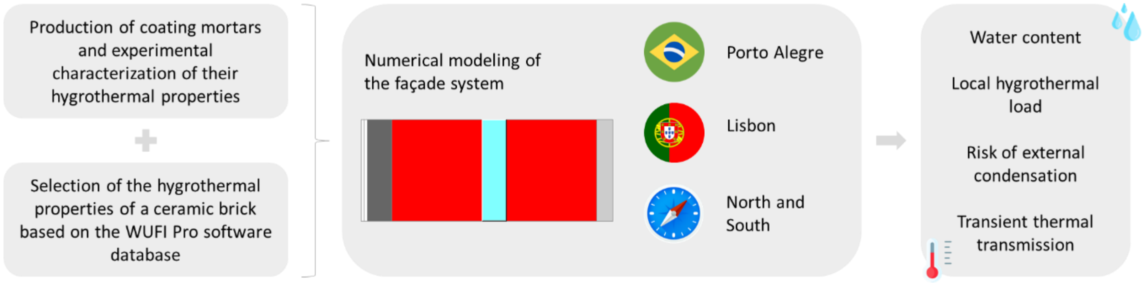


**Source:** Freepik resources from Flaticon.com.

Neglecting moisture dependency was assumed due to the unavailability of own experimental data; uncertainties may result from this assumption, especially by underestimating heat transfer in humid materials. Nevertheless, this approach accounts for most standards that present fixed conductivity values for normalized conditions (Gomes *et al.*, 2017). The thermal efficiency of the wall was potentially improved by assuming a fully sealed or very weakly ventilated cavity (Gagliano; Aneli, 2020), as thermal resistance can be significantly reduced by openings on the bottom and top of the walls. Finally, indoor climate conditions were assumed to be standardized, allowing for the isolation of the influence of exterior climate conditions on the results, regardless of indoor temperature and relative humidity conditions.

In this work, the terms "transmittance" and "transmission" are used to describe the properties of the building component, corresponding to the rates of heat or moisture transmission under constant boundary conditions. In contrast, the expressions "transfer" and "transport" refer to transient physical processes that involve time-dependent conditions. This distinction ensures conceptual consistency with the terminology adopted in ISO 12572 (ISO, 2016) and ISO 13786 (ISO, 2015).

## 2.1 Materials

The evaluated façade system, shown in Figure 3, consists of a double ceramic brick wall with an air cavity, internally and externally coated with mortars. This reflects the construction practice of the 1990s in Portugal (Sousa, 2000). For Brazil, to ensure a fair and conservative comparison, the double wall was selected, even though typical Brazilian masonry uses only one ceramic brick leaf about 14 cm thick (Corrêa, 2012), and housing in the southern region is generally poorly insulated (Rodrigues; Parente; Fernandes, 2024). Since construction technology has a notable impact on the energy performance and economic feasibility of nearly zero-energy buildings (nZEB) (Teni; Čulo; Krstić, 2019), using a double-wall approach enables a consistent comparison of energy demands between the two places.

Properties for the numerical simulation were experimentally determined by the authors for the thermal and base coat mortars used as external rendering, and for the lime-based conventional mortar, applied as an internal plaster. The fiberglass mesh, traditionally inserted between two layers of base coat, was disregarded in the simulations.

Figure 3 - **Façade system and its layers**

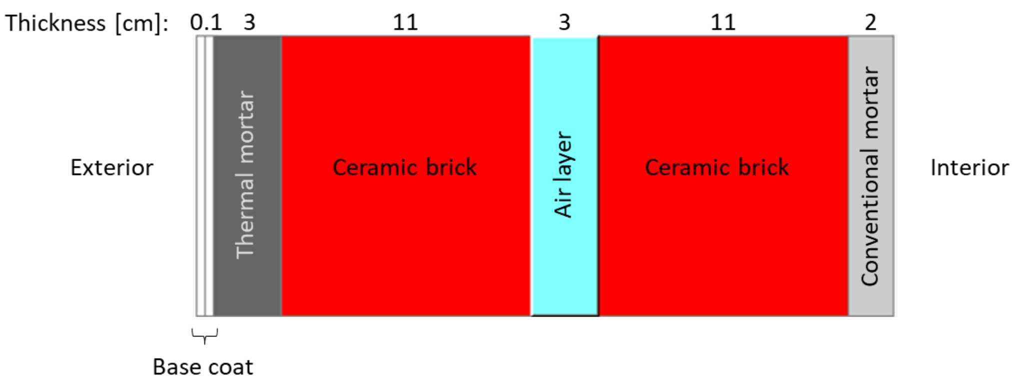

The tested mortars are supplied dry-mixed by the manufacturer and made with natural hydraulic lime. The base coat contains binders and cork aggregates. The thermal mortar is lightweight, with additions, expanded cork and limestone aggregates. The conventional mortar contains siliceous and limestone aggregates. Figure 4 illustrates the production and characterization of these mortars in both fresh and hardened states, highlighting their hygrothermal properties, including open porosity, hygroscopic curves, capillary absorption, vapor transmission, and thermal conductivity.

The mortars were mixed in the laboratory, using an Automix Controls mixer, following NP EN 196-1 (IPQ, 2006): slow speed for 60 seconds, fast speed for 30 seconds, standstill for 90 seconds, and then fast speed for 60 seconds. The maximum water contents recommended by the manufacturer were added during production by the authors: 325 cm³ of water/kg of the base coat dry mix, 500 cm³/kg for the thermal mortar, and 150 cm³/kg for the conventional mortar. Thus, with the Flow Table test following EN 1015-3 (ECS, 1999), consistency indices of 150 ± 10 mm (base coat), 160 ± 10 mm (thermal mortar), and 170 ± 10 mm (conventional mortar) were obtained.

Hygroscopic curves were determined for the mortars in accordance with ISO 12571 (ISO, 2013), and Figure 5 presents the adsorption results. The specimens were exposed to relative humidities of 10%, 33%, 50%, 75%, and 95%. Other hygrothermal properties and their determination methods are summarized in Table 1. Water vapor permeability was tested in a climatic chamber with a temperature of 23 °C and a relative humidity of 50%. Water absorption coefficients were determined using the values obtained after 10 and 90 minutes of testing. Reference water content was determined based on the adsorption curves.

The thermal conductivity of the mortars was determined using the transient method with an ISOMET 2114 equipment. Unfortunately, dependencies between water vapor permeability and thermal conductivity with respect to variations in temperature and relative humidity were not experimentally characterized and, therefore, were not included in the simulations. Specific heat capacity was not experimentally determined but was adopted from typical values found in the WUFI Pro 7.1 database for lime-based mortars and previously used in other studies (FIBP, 2019; Posani; Veiga; Freitas, 2022).

For the ceramic brick, database values (FIBP, 2019) were used for unaged aerated clay bricks. The specific heat capacity of the brick was shown with the same value as for the mortars, 850 J/(kg.°C); according to the WUFI Pro 7.1 manual (FIBP, 2019), this is a rough value adopted for mineral materials, considered sufficient since hygrothermal simulations typically are not sensitively affected by this property.

Figure 4 – **Mortars' production and characterization**

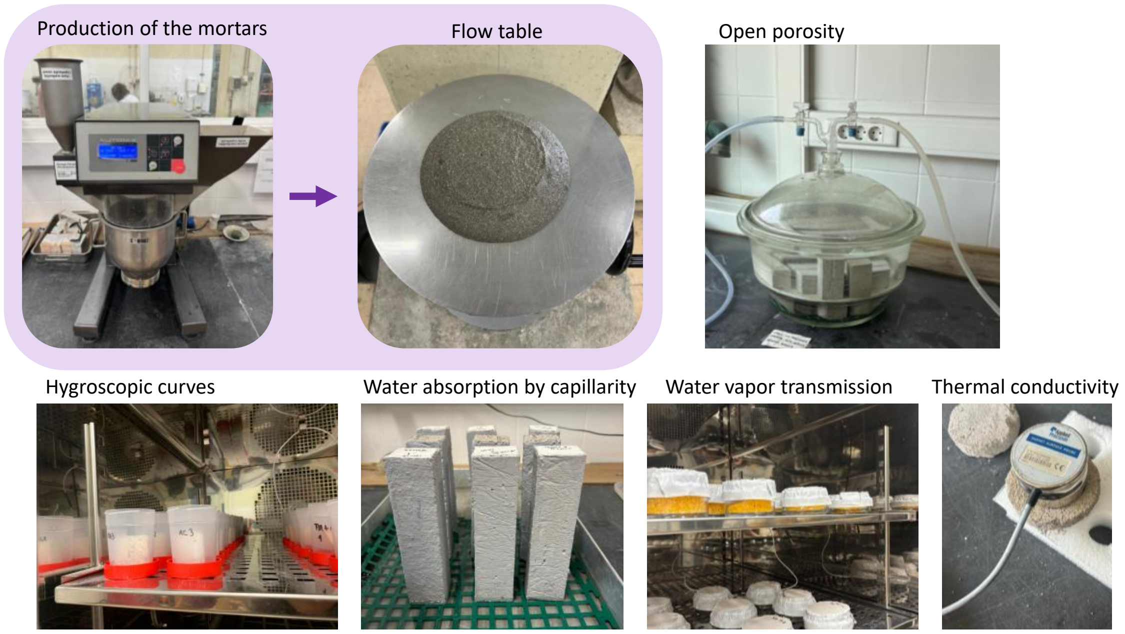

## 2.2 Methods

The numerical simulations aimed to calculate non-steady heat and moisture transport processes in the one-dimensional, multi-layered assembly depicted in Figure 3, using WUFI Pro 7.1. For that, the differential Equations 1 and 2 were solved for heat and moisture transport, respectively (FIBP, 2019):

$$\frac{\partial H}{\partial \vartheta}\frac{\partial \vartheta}{\partial t} = \frac{\partial}{\partial x}\left(\lambda \frac{\partial \vartheta}{\partial x}\right) + h_V \frac{\partial}{\partial x}\left(\frac{\delta}{\mu}\frac{\partial p}{\partial x}\right) \quad \text{Eq. 1}$$

$$\rho_W \frac{\partial u}{\partial \varphi}\frac{\partial \varphi}{\partial t} = \frac{\partial}{\partial x}\left(\rho_W D_W \frac{\partial u}{\partial \varphi}\frac{\partial \varphi}{\partial x}\right) + \frac{\partial}{\partial x}\left(\frac{\delta}{\mu}\frac{\partial p}{\partial x}\right) \quad \text{Eq. 2}$$

Where:

$D_W$ is the liquid transport coefficient (m²/s);

H is the enthalpy of moist building material (J/m³);

$h_V$ is the evaporation enthalpy of water (J/kg);

p is the water vapor partial pressure (Pa);

u is the water content (m³/m³);

$\delta$ is the water vapor diffusion coefficient in air (kg/(m.s.Pa));

$\vartheta$ is the temperature (°C);

$\lambda$ is the heat conductivity of moist material (W/(m.K));

$\mu$ is the vapor diffusion resistance factor of dry material (non-dimensional);

$\rho_W$ is the density of water (kg/m³); and

$\varphi$ is the relative humidity (non-dimensional).

In Equations 1 and 2, the left-hand terms represent storage, while the right-hand terms reflect transport. For heat storage, both the heat capacity of the dry material and the moisture present within it are taken into account. Then, heat transport includes moisture-dependent thermal conductivity and vapor enthalpy flow resulting from the latent heat effect. Liquid transport encompasses surface diffusion and capillary conduction, which occur due to a relative humidity gradient, with a slight dependence on temperature. Differently, vapor diffusion saturation pressure increases exponentially with temperature (FIBP, 2019).

Figure 5 - **Hygroscopic adsorption curves**

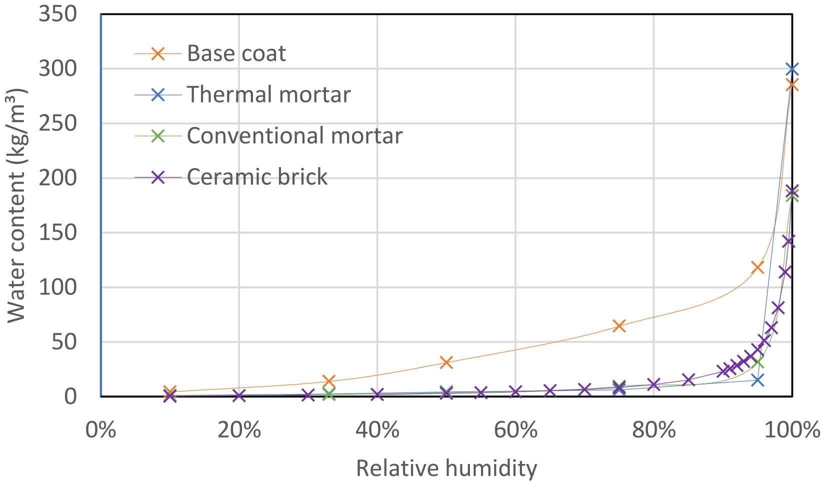


**Source**: the authors and, for the ceramic brick, WUFI Pro 7.1 database (FIBP, 2019).

Table 1 – **Material properties**

| Property | Mortars | | | | Ceramic brick |
|---|---|---|---|---|---|
| | Base coat | Ther-mal | Conventional | Standards/ Methods | |
| Bulk Density (kg/m³) | 1116 | 666 | 1579 | EN 1015-10 (ECS, 1999) | 600* |
| Open Porosity (m³/m³) | 0.3761 | 0.5854 | 0.2582 | NP EN 1936 (IPQ, 2008) | 0.77* |
| Specific Heat Capacity (J/(kg.°C)) | 850* | 850* | 850* | - | 850* |
| Thermal Conductivity (W/(m.°C)) | 0.19 | 0.08 | 0.43 | ASTM D7984 (ASTM, 2021) | 0.12* |
| Water Vapor Diffusion Resistance Factor (-) | 14.19 | 9.06 | 14.02 | ISO 12572 (ECS, 2016) – silica gel | 16* |
| Reference Water Content (kg/m³) | 77.89 | 8.38 | 14.99 | ISO 12571 (ISO, 2013) | 11* |
| Free Water Saturation (kg/m³) | 285.42 | 299.53 | 183.87 | EN 1015-18 (ECS, 2002) | 188* |
| Water Absorption Coefficient (kg/(m².√s)) | 0.018 | 0.022 | 0.016 | EN 1015-18 (ECS, 2002) | Liquid Transport Coefficient – Suction/ Redistrib.: 11kg/m³ - $2.5E^{-10}$ m²/s; 188kg/m³ - $1.22E^{-6}$ m²/s and $1.3E^{-6}$ m²/s* |

**Source:** the authors and WUFI Pro 7.1 database (FIBP, 2019).

**Note:** properties indicated with * were adopted from the WUFI Pro 7.1 database (FIBP, 2019); other properties were obtained experimentally.

Hygrothermal simulations require definitions of components, assemblies, initial conditions, and boundary conditions for exterior and interior climates. Section 1.1 lists all parameters input for materials, including thickness and properties. Initial conditions were set at 80% relative humidity and a temperature of 20 °C.

Table 2 presents the boundary conditions adopted for the 4-year numerical simulations. The simulations lasted 4 years to allow for the conditioning period to be completed, ensuring that the effect of the initial conditions was completely eliminated from the final assessments (Vandemeulebroucke *et al.*, 2023). The software's default values for thermal resistances, ground reflectivity, and incident rain reduction factor were not modified, as they are suitable for the wall assembly (FIBP, 2019).

The explicit radiation balance and long-wave emissivity were actively considered to include potential excessive surface cooling and radiative heat loss. This consideration was especially important in assessing exterior surface condensation. Such condensation occurs when the exterior surface temperature drops below the dew point. This condition results from the exchange of long-wave radiation between the surface and the atmosphere. It is intensified on clear nights, when the surface emits more radiation than it receives, resulting in a net loss to the sky (Barreira; Freitas, 2014).

Table 3 and Figure 6 present the main climatic parameters for Porto Alegre and Lisbon. For Porto Alegre, data from INMET (2018) were used, while for Lisbon, software default conditions (FIBP, 2019) were adopted. As Figure 6 illustrates, the highest solar radiation sums for the two cities occur in opposite directions, reflecting their latitudinal differences; yet the dominant wind-driven rain orientations are similar.

The indoor climate was simulated according to EN 15026 (ECS, 2023), with indoor air temperatures higher than 20 °C for outdoor temperatures lower than 10 °C, but limited to 25 °C for outdoor temperatures higher than 20 °C. Moisture production was assumed to be normal.

After running the simulations, the hygrothermal performance was analyzed. Firstly, the total water content throughout time was extracted for the entire cross-section under different exposure conditions. Although the level of total water content depends on the thickness of the assembly, as it was fixed across the simulations, the results allow for an accurate comparison. For the most critical scenario, water contents were analyzed individually by layer to discriminate the system's behavior and understand if the absolute amount of water in the materials was acceptable.

Local hygrothermal loads were assessed for the interior surfaces of the four types of simulation: two locations (Porto Alegre and Lisbon) and two orientations (north and south). These loads are graphically represented as combinations of relative humidity and internal surface temperature at the time steps used in the simulation. This parameter can be plotted against limiting isopleths for construction materials, indicating conditions that favor the potential development of mold. Limit B II was selected for this study, corresponding to porous substrates such as plaster and mineral materials, provided they are not pre-contaminated. If the conditions lie above the limiting isopleths for a long enough period, mold growth may be possible (FIBP, 2019).

The external condensation risk was assessed based on the number of hours the external surfaces of the façades presented 100% relative humidity (Pedroso *et al.*, 2023; Ramos *et al.*, 2014); for this, the obtained relative humidity values were rounded to the nearest integer. Interstitial condensation was also investigated by assessing the dynamic fluctuation of heat and moisture transport throughout time across the façade assembly, an output from WUFI Pro 7.1 in the form of a video (FIBP, 2019). Interstitial condensation occurs when the temperature along the cross-section lies below the dew point (Squadroni *et al.*, 2022).

Table 2 – **Boundary conditions**

| Condition | Value |
|---|---|
| Orientation | North and South |
| Inclination | 90° |
| Building Height | Tall building, middle part, up to 10–20 m |
| Exterior Heat Resistance | 0.0588 (m².°C)/W |
| Exterior sd-Value | 0.01 m (Silicate paint) |
| Short-Wave Radiation absorptivity | 0.2 (Stucco, White (new)) |
| Ground Short-Wave Reflectivity | 0.2 |
| Ground Long-Wave Emissivity | 0.9 |
| Ground Long-Wave Reflectivity | 0.1 |
| Adhering fraction of rain | 0.7 |
| Interior Heat Resistance | 0.125 |
| Interior sd-Value | 0.01 m (Silicate paint) |

**Source**: WUFI Pro 7.1 database (FIBP, 2019).

Table 3 – **Climatic conditions**

| Parameter | Porto Alegre | Lisbon |
|---|---|---|
| Mean Temperature (°C) | 20 | 15.6 |
| Maximum Temperature (°C) | 37.4 | 37 |
| Minimum Temperature (°C) | 2.8 | 1.2 |
| Mean Relative Humidity (%) | 74 | 74.6 |
| Maximum Relative Humidity (%) | 96 | 100 |
| Minimum Relative Humidity (%) | 23 | 25 |
| Mean Wind Speed (m/s) | 1.5 | 3.9 |
| Normal Rain Sum (mm/a) | 1168 | 674.9 |
| Cloud index (-) | 0.64 | 0.66 |

**Source**: INMET (2018) and WUFI Pro 7.1 database (FIBP, 2019).

Figure 6 - **Solar radiation and wind-driven rain sums in Porto Alegre and Lisbon**

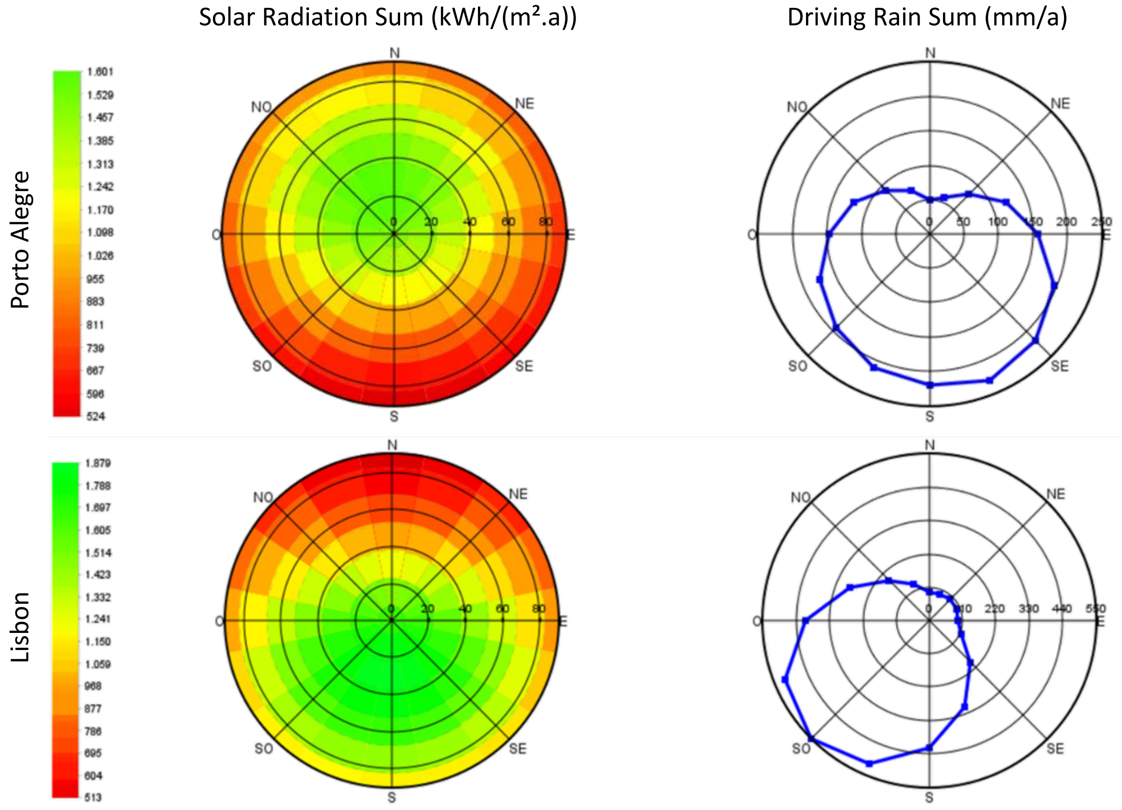


**Source:** INMET (2018) and WUFI Pro 7.1 database (FIBP, 2019).

The transient thermal transmittance of the façade systems was estimated using the method provided in the Thermal Transmission 2.3.1 post-processing tool, developed to evaluate heat losses. Under steady-state conditions, the thermal transmittance of an envelope component remains constant and can be determined using Equation 3 (ISO, 2017).

$$U = \frac{\phi}{(T_1 - T_2)A} \quad \text{Eq. 3}$$

Where:

U represents the thermal transmittance (W/m$^2$.°C);

ϕ is the heat flow rate, i.e., the quantity of heat transferred through the system per unit time (W);

A is the analyzed area (m$^2$); and

$T_1$ and $T_2$ are the temperatures on both sides of the envelope (°C).

In contrast, under transient thermal conditions, the heat transfer process becomes time-dependent due to variations in external temperature, solar radiation, and boundary conditions. Both sensible and latent heat fluxes vary over time, leading to temporary heat storage and release within the layers, and causing the apparent thermal transmittance to fluctuate. This dynamic behavior is governed by the properties of the materials, specifically thermal conductivity, specific heat capacity, density, and layer thicknesses, which determine both the rate of heat propagation and the system's ability to store thermal energy.

The monthly transient thermal transmittance values were obtained from simulation results considering the moisture content determined by WUFI Pro 7.1 (FIBP, 2019) and calculated using Equation 4. The transient thermal transmittance may account for material properties that vary with moisture, additional heat sources (such as solar radiation), and environmental conditions (including surface heat coefficients that depend on wind) (Flood; Scott; Gleeson, 2016).

$$U_M = \frac{-Q_{1,M}}{(\vartheta_i - \vartheta_a)_M} \quad \text{Eq. 4}$$

Where:

$U_M$ represents the monthly transient thermal transmittance values (W/m².°C);

$Q_{I,M}$ is the monthly average heat flux density through the internal surface (W/m²); and

$(\vartheta i\text{-}\vartheta a)_M$ is the monthly average temperature difference between indoor and outdoor air (°C).

Equation 4 properly reflects the definition of ISO 13786 (ISO, 2015) for periodic thermal transmittance, as a complex quantity determined by dividing the amplitude of the density of the heat flow rate by the amplitude of the temperature. $U_M$ results were compared with the maximum allowable thermal transmittance for vertical envelopes in Porto Alegre (bioclimatic zone 2R (ABNT, 2024)), 2.7 W/(m²·°C) (ABNT, 2021), and Lisbon, 0.50 W/(m²·°C) (República Portuguesa, 2021).

## 3 Results and discussion

Figure 7 shows the total water content series per unit area of façade over the simulation years for Porto Alegre and Lisbon. In line with the annual sum of driving rain shown in Figure 6, both cities exhibit higher water contents on the south-facing façades.

The north façade of Porto Alegre shows only slight variation in water content throughout the year. Peak values are about 1.0 kg/m² higher than the minimum, which is just below 2.0 kg/m². These values are somewhat higher than those seen by Bersch *et al.* (2024) for façades coated with satin acrylic paint, conventional lime mortars, and a simple ceramic brick wall in Porto Alegre. In the one leaf wall (a single-layer wall without insulation), however, less pronounced differences were observed between orientations (Bersch *et al.*, 2024).

Figure 7 - **Total water contents per unit area throughout time for: (a) Porto Alegre; (b) Lisbon**

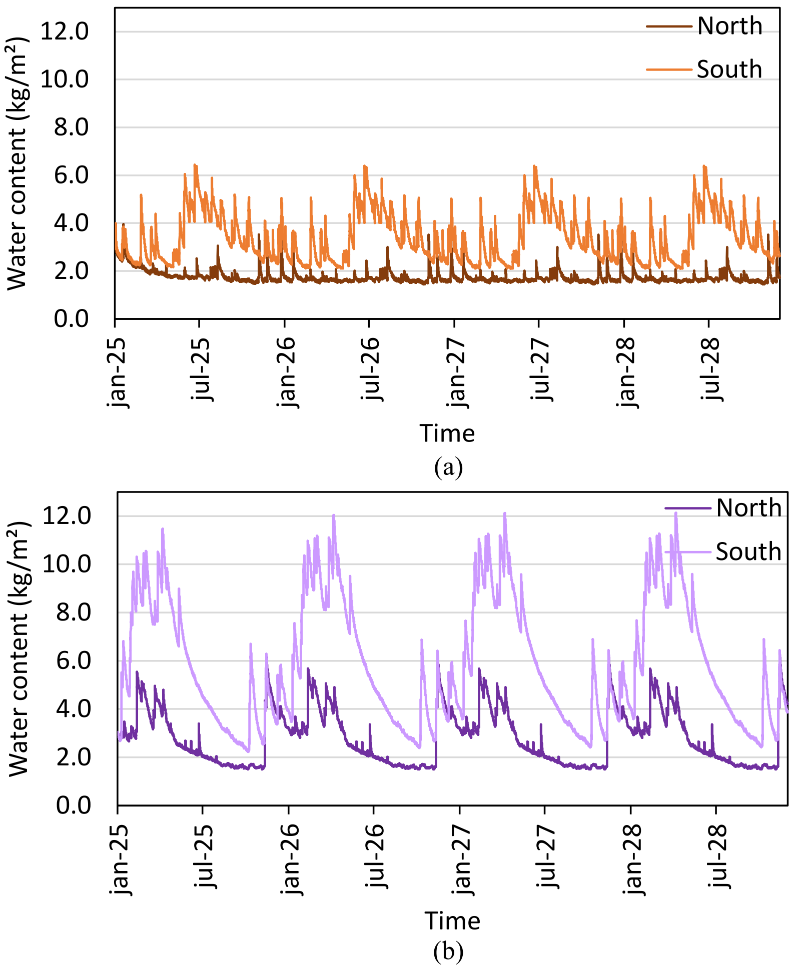

On the other hand, the moisture content values in Porto Alegre (Figure 7(a)) are similar to those obtained by Kleber (2018) for simple ceramic brick walls with conventional mortar coatings and without paint. This matches the fact that the external surface's water absorption coefficient by capillarity remained unchanged in the present research, despite the potential for paint finishing to reduced it. Indeed, Baltazar and Morais (2023) found an 89% reduction in that coefficient for renders with silicate paint, although the drying process remained mostly unaffected. Lisbon, on the other hand, is more severely affected by moisture, as shown in Figure 7(b). The values presented by its north façade, which exhibits the lowest moisture content, are comparable to the highest ones for Porto Alegre (north façade), with maximum peaks roughly half those observed on the south façade in Lisbon.

The low variations in total water contents of façades oriented towards the north in Porto Alegre are due to the low exposure to wind-driven rain loads in this orientation throughout the year, with a yearly sum of 50 mm. The south orientation receives four times more impinging rain throughout the year, which is still half of the rain that falls on the southern walls in Lisbon. As the climate files for both cities were provided for one typical year, the weather parameters are repeated annually from 2025 to 2028; they do not reflect differences in weather conditions throughout the period. Thus, the graphs also show repeating results after 2026, indicating that a dynamic steady state is reached from the second year onward; this is important because the initial conditions no longer influence the observed results.

Figure 8 presents the water content in mass percentage per layer for the south façade in Lisbon, which was selected as the most critical situation due to its highest total water content, as shown in Figure 7. The mass percentage represents the ratio between water mass and dry material mass. Among all the layers from the façade assembly, the thermal mortar has the highest moisture content, especially during the winter months (December to March). The high open porosity of the thermal renders helps explain this behavior, as reflected in faster water absorption (Posani; Veiga; Freitas, 2022) and an increased capacity for water storage. Maia, Ramos and Veiga (2018) attribute the high water absorption coefficients of thermal renders to their high rate of mesopores (capillary network), which leads to relevant moisture content during the lifetime of buildings.

The base coat mortar comes in second place regarding water content, measured as a percentage by mass, due not only to its proximity to the external environment but also to its hygroscopic nature, which stores higher moisture contents than the other materials for relative humidity above 40%, as indicated by the adsorption curves in Figure 5.

Moisture in the thermal mortar indicates the behavior of the base coat. This coat lets water reach the insulation layer. Fino, Tadeu, and Simões (2018) report that neglecting the water absorption coefficient can lead to incorrect results, especially when façades are exposed to heavy wind-driven rain. The present simulations did not consider any reduction of the base coat mortar's water absorption coefficient due to the silicate paint's capillarity; thus, the simulations remain conservative.

Figure 8(b) shows that the remaining layers maintain a water content below 2% throughout the year, except for the external ceramic brick, which reaches 6%. These moisture levels can be considered acceptable (below 4% (Krause; Pokorska-Silva; Kosobucki, 2025). The conventional mortar had the lowest water content, as the internal plaster does not come into contact with weather conditions, and the simulations used normal indoor moisture loads.

Figure 9 shows local hygrothermal loads for the wall in both locations and orientations. Yellow points represent early simulation steps that are still influenced by initial conditions. Final assessments use darker points, indicating dynamic balance. The internal surface's relative humidity and temperature remain below the threshold for mold growth, matching the water contents shown in Figure 8.

The façade assembly of the double ceramic brick wall is designed for improved thermal inertia (Martínez-Sala *et al.*, 2025) compared to traditional single-leaf masonry, which may have contributed to the relatively similar performance across the four cases shown in Figure 9. Kleber (2018) identified the risk of mold growth for a simple brick wall coated with external and internal cement and natural hydraulic lime mortar, as well as acrylic paint (sd-value of 0.5 m) in Porto Alegre. For a single-leaf wall with external and internal mortar coatings in Pelotas, a city with a humid subtropical climate, Buligon *et al.* (2022) identified risks of mold growth on the interior surface, both with natural and artificial ventilation, for north and south orientations. Similar conclusions were reported by Beber *et al.* (2024). In Pelotas, wind-driven rain loads reach 740 mm annually in the south, which is higher than in Porto Alegre and Lisbon. Ventilation was not considered in the air cavity in this study, which could have influenced the results if inadequate, leading to insufficient drying and facilitating moisture defects when combined with high relative humidity and low sun exposure (Ingebretsen *et al.*, 2022). Therefore, more demanding climate conditions should be examined to compare single- and double-leaf walls, thereby clarifying their impact on mold growth.

Figure 8 – **Water content per layer in mass percentage throughout time for the south façade in Lisbon**

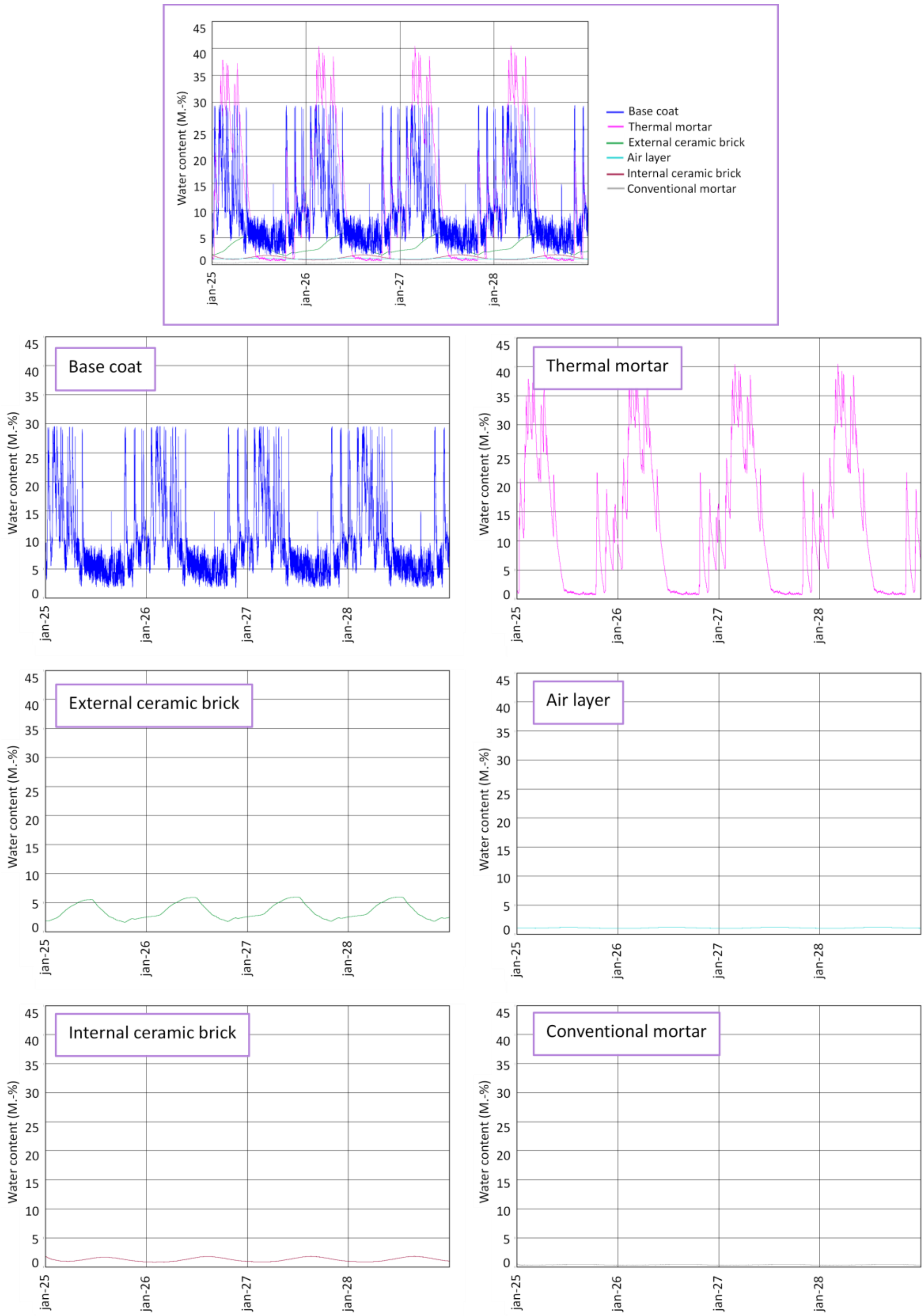

Figure 9 - **Local hygrothermal loads for: (a) Porto Alegre - North; (b) Porto Alegre - South; (c) Lisbon - North; (d) Lisbon - South**

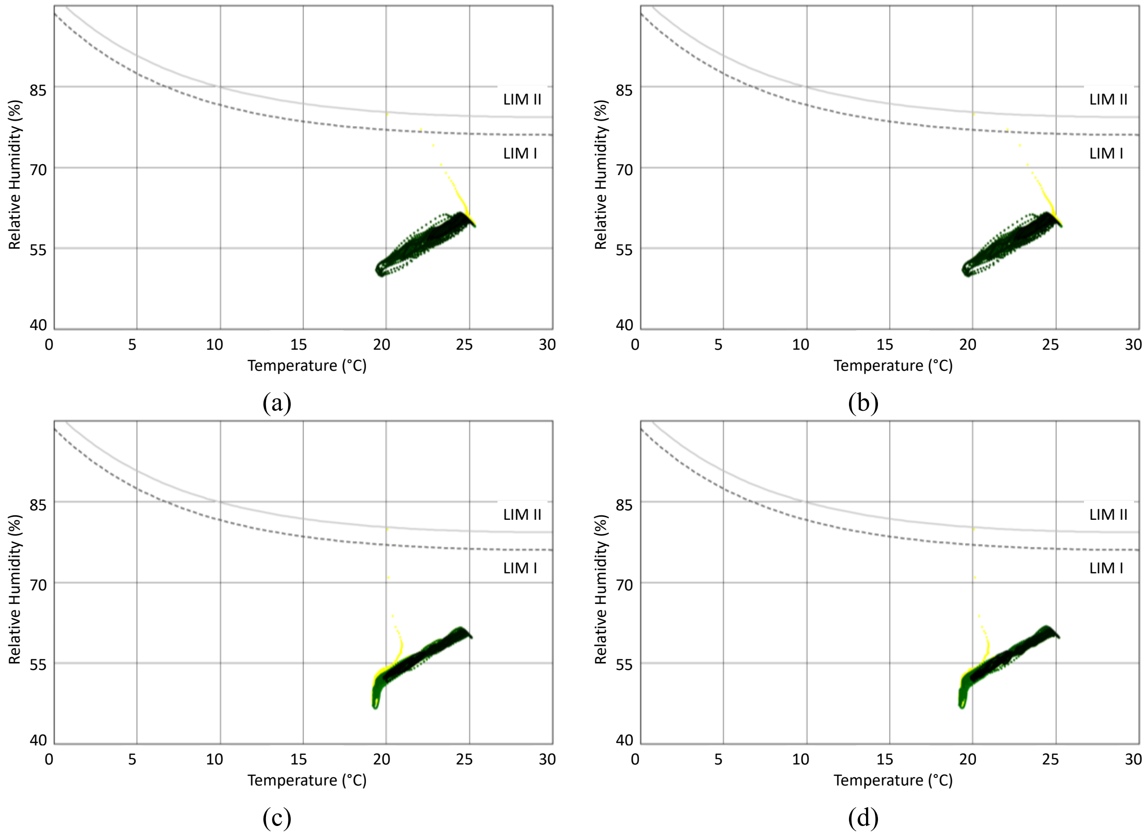


Figure 10 compiles the results of relative humidity and temperature at the external surfaces. The plotted values are not averaged, allowing dynamic amplitudes to be checked and absolute values to be quantified. As expected, the highest temperature peaks occur around January in Porto Alegre and July in Lisbon, thus, during the respective summer periods. The highest and lowest temperature values are rather similar between cities.

Numerical analysis of Figure 10 shows condensation risk for Porto Alegre façades: 41 hours on the north, 212 on the south. Because south-facing façades in the Southern Hemisphere receive less solar radiation, they experience reduced evaporation and increased condensation, favoring microbial growth (Sato *et al.*, 2008). This occurred in the Château, a historic building in Porto Alegre, rendered with conventional lime-based mortar (Verdum *et al.*, 2021).

In Lisbon, 162 and 702 hours with a surface relative humidity of 100% were recorded on the north and south façades, which account for 0.5% and 2% of the total simulation period. Figure 10 shows a higher risk of external condensation in Lisbon during winter. For this assessment, the sd-value was used to evaluate how silicate paint affected water vapor permeability and the potential accumulation of condensation moisture (Šadauskienė *et al.*, 2009) by reducing the vapor transferred through the façade system (Karoglou *et al.*, 2013). However, because the sd-value of silicate paints is low, its influence on condensation was probably minor (Šadauskienė *et al.*, 2009). Additionally, since silicate paints generally do not lower water absorption as much as other paints, such as silicone-based ones, they may retain the least water condensation on the surface (Künzel, 2007). Therefore, the observed effects are mainly due to the mortar render itself.

Parracha *et al.* (2024a) also observed external condensation in thermal mortars with expanded polystyrene (EPS) and aerogel aggregates (thermal conductivities of 0.042–0.050 W/(m·°C) and 0.029 W/(m·°C), and densities of 150–200 kg/m³ and 165 kg/m³, respectively) exposed to natural aging in Lisbon, especially on north-facing façades. Pedroso *et al.* (2023) also identified a condensation potential for aerogel-based thermal mortars (density ~160 kg/m³) in Lisbon, studying materials with lower thermal conductivities than classical insulating materials like EPS; hours with 100% external surface relative humidity in new constructions covered at least 1.8% of the simulation time, similar to the value observed in this study for the north.

Figure 10 - **Exterior surface relative humidity and temperatures over simulation time Porto Alegre - North**

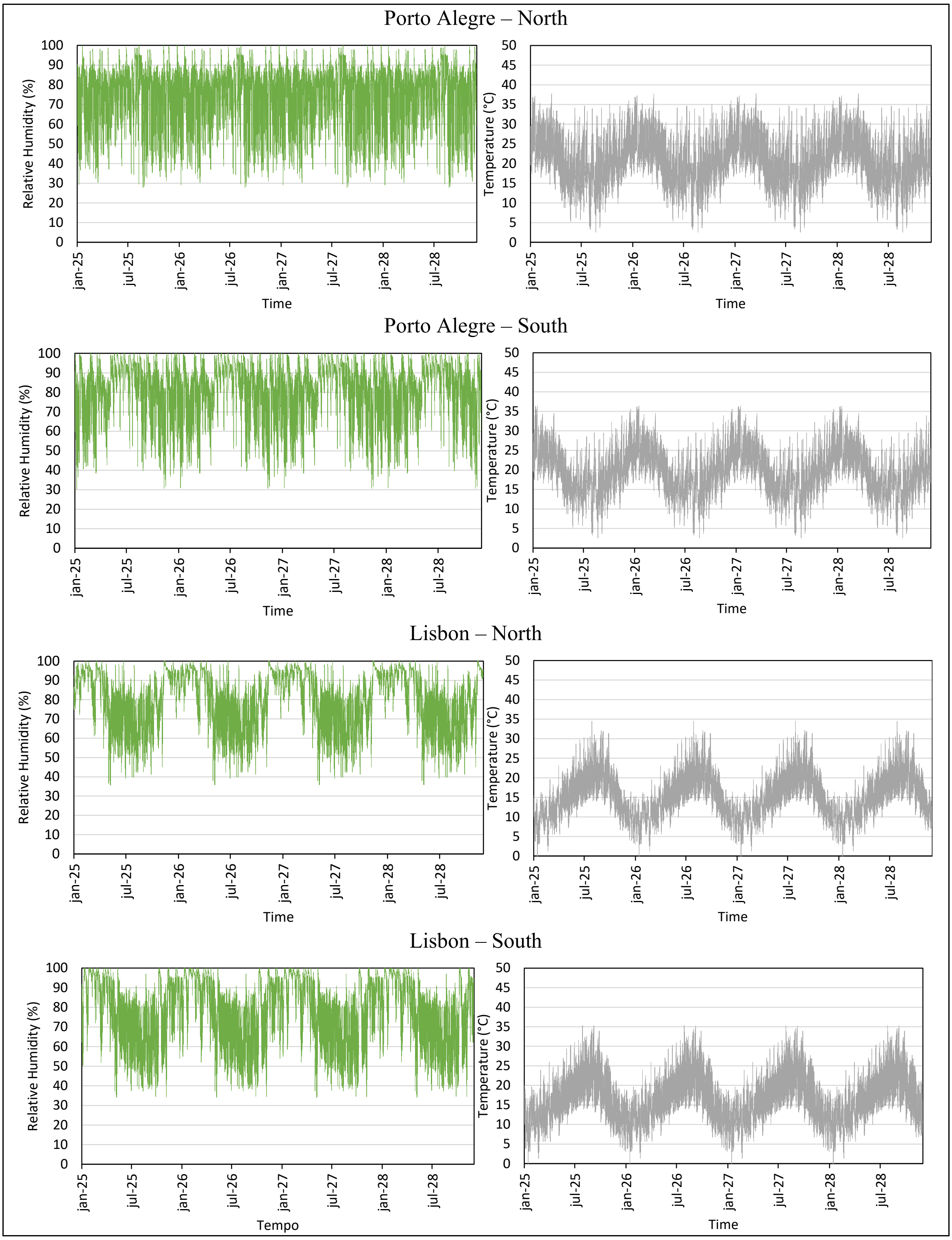


Thermal mortars should typically exhibit lower condensation compared to ETICS panel systems, since they also provide lower thermal insulation capacity. In the case of ETICS panel systems, the computation of 100% relative humidity hours on the external surface, as determined through simulation results, was underestimated when compared with monitoring using sensors (Parracha *et al.*, 2024b).

Regarding interstitial condensation, analysis of cross-section profiles over time revealed possible episodes in the thermal mortar layer in Porto Alegre and Lisbon, especially on south-facing façades. Figure 11 shows a winter day example on south-oriented walls, where temperature and dew point lines overlap in the external coating mortars. This overlap confirms concerns about the thermal inertia of the cladding, which leads to external condensation (Künzel, 2007). These findings underscore the importance of effective surface protection. Additionally, condensation in the insulation layer harms thermal conductivity, promotes fungal and biological growth, and alters the thermophysical properties of materials (Tronchin; Fabbri; Tommasino, 2023).

Even so, composite layers, such as mortared joints, used as an external finish for masonry, may reduce the risk of interstitial condensation, especially when cavity walls are insulated, thereby fostering drying (Hens, 2006). Indeed, placing thermal insulation materials on the inside surface results in even higher condensation risks if compared to their addition to the exterior (Baran *et al.*, 2016).

Finally, Figure 12 shows the average monthly transient thermal transmittance values for the façade systems. In Lisbon, the profile is relatively uniform throughout the year, with higher values around July for the south façade due to higher internal surface temperatures compared to external ones. In Porto Alegre, pronounced peaks occur near summer months, likely reflecting numerical adjustments during the transition period when heat flux reverses direction from exterior to interior.

According to Figure 12, thermal transmittance in Lisbon for north-facing façades met both Lisbon and Porto Alegre requirements throughout the simulation period, with $U_M$ values below 0.50 W/(m²·°C) (Portaria No 138-I/2021 (República Portuguesa, 2021)) and 2.7 W/(m²·°C) (NBR 15575-4 (ABNT, 2021)). For south-facing façades, the 0.50 W/(m²·°C) limit was exceeded in summer months. In Porto Alegre, the results met the maximum allowed value of 2.7 W/(m²·°C) (ABNT, 2021) for both orientations (considering peaks as numerical adjustments). However, the system could not reach a value lower than 0.50 W/(m²·°C) on the south façade.

Figure 11 - **Interstitial condensation risk on a winter day for the south façade in: (a) Porto Alegre; (b) Lisbon**

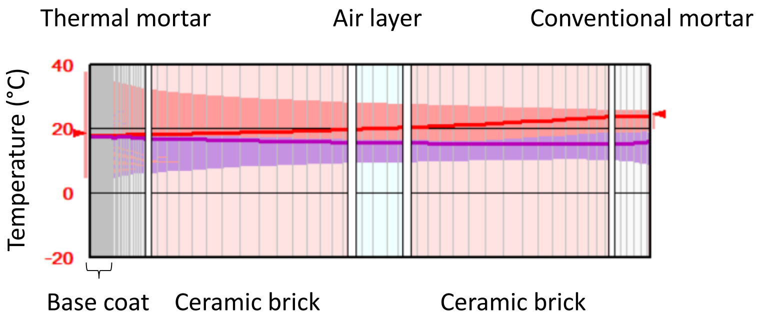


(a)

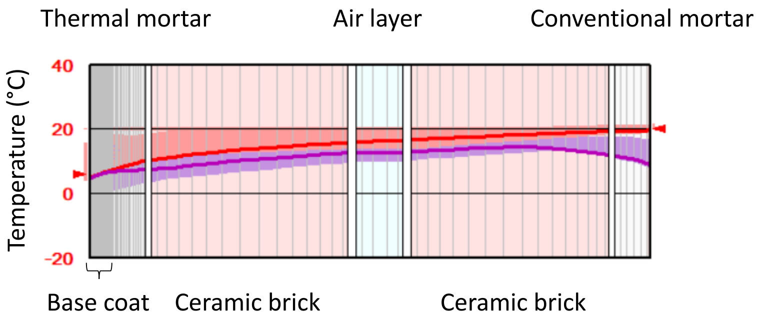


(b)

**Note:** red: temperature on the cross-section; purple: dew point temperature.

Figure 12 - **Average monthly transient thermal transmittance for: (a) Porto Alegre; (b) Lisbon**

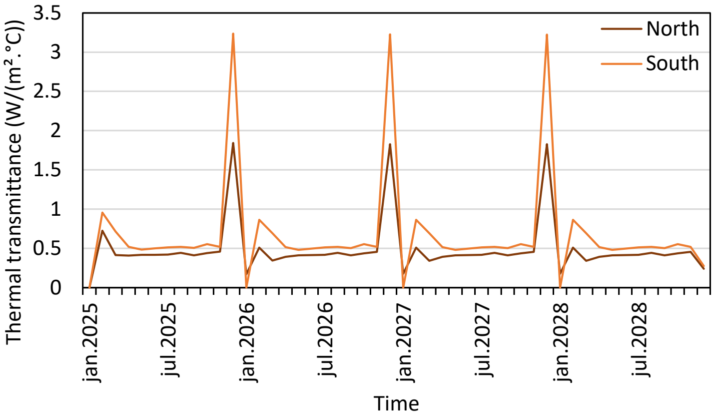


(a)

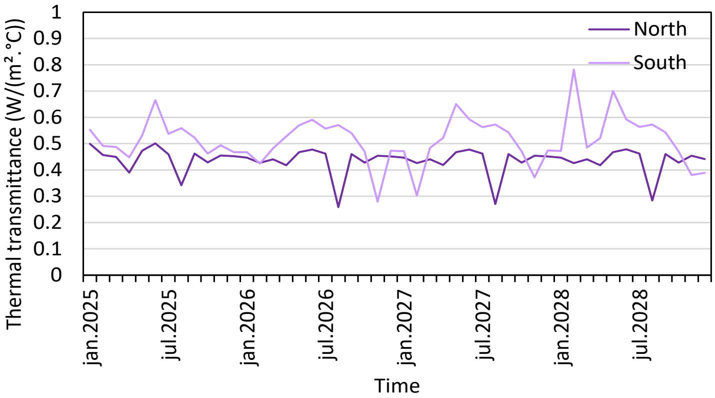


(b)

A limitation of the hygrothermal simulations was that the dependency between mortar thermal conductivity and relative humidity was not included, which could have intensified heat transfer, especially following condensation results. Posani, Veiga and Freitas (2022) identified thermal conductivities of 0.098 W/(m·°C) and 0.325 W/(m·°C) for cork-aggregate thermal mortar in dry and saturated states, respectively. Furthermore, the interior climate was tested with temperatures ranging from 20 °C to 25 °C, and relative humidities from 30% to 60%; however, these comfort conditions are not accomplished at least over 50% of the winter in Southern European countries (Ranesi *et al.*, 2022). Optimization of the simulated conditions is, therefore, still required. Despite this, stationarity can also be considered a periodic regime with temperatures varying cyclically over time; for this reason, Parracha *et al.* (2023) obtained slightly lower results for mortars applied to a prototype wall subjected to a heat flux compared to a conventional thermal conductivity transient test.

Considering that the studied façade system is similar to technologies used in Portugal in the late 1990s (Sousa, 2000), the transient thermal transmittance results could be pointed as adequate for the rehabilitation of existing Portuguese residential buildings, with a recommended maximum U-value of 1.7 W/(m²·°C) (Portaria Nº 297/2019 (República Portuguesa, 2019)). For Porto Alegre, this rehabilitation requirement is also accomplished. Furthermore, if an additional scenario were simulated, replacing the external thermal render with the same conventional mortar applied as interior plaster, the thermal conductivities would differ for the whole façade system, with an increase of almost 15%, which would also influence transient results. Indeed, lower heat fluxes correspond to mortars with lower thermal conductivities (Parracha *et al.*, 2023).

However, a remark should be made if the simulation explicitly aimed to address existing buildings: in this case, besides typical operation conditions, higher initial water contents in the substrate may need to be considered (Posani; Veiga; Freitas, 2023). Indeed, for thermal and energy retrofits, moisture contents resulting from interventions must be taken into account to mitigate the risk of pathologies such as mold development and material degradation (Martín-Garín *et al.*, 2021).

# 4 Conclusions

This study evaluated the hygrothermal performance of a masonry façade system with a double wall and air cavity, externally coated with a multilayer insulation system with thermal mortar. The focus was devoted to moisture contents, local hygrothermal loads, external condensation potential, and transient thermal transmittance. Experimentally obtained data were used for three types of mortars based on natural hydraulic lime, with the thermal mortar being lightweight and enhanced with expanded cork aggregates.

Total moisture contents on north- and especially south-facing façades in Lisbon were much higher than those observed in Porto Alegre, where the façade with the highest driving rain exposure had peaks similar to the façade with lower exposure in Lisbon. In the most critical case, Lisbon, south façade, the base coat and thermal mortar layers were primarily responsible for the identified moisture contents. As these are the outermost layers, the importance of external surface protection becomes evident, and further simulations are recommended to consider the potential reduction in capillary water absorption due to silicate paint application.

Despite the moisture in the external layers, the internal layers exhibited acceptable values throughout the simulation period. Based on the assessment of local hygrothermal loads, no potential issues regarding mold development on internal surfaces were identified. It is worth noting that the simulation considered a double wall with an air cavity, providing increased thermal inertia compared to single-leaf wall systems.

Regarding external surface condensation, the risk was proportional to the moisture content for each façade. North-facing façades exhibited a lower risk than south-facing ones in both cities, with Lisbon showing three to four times higher risk based on the number of hours when the external surface relative humidity reached 100%. Additionally, condensation risk extends from the surface into the thermal mortar layer, potentially reducing its insulation performance. This again highlights the importance of considering capillary water absorption protection and characterizing thermal conductivity coefficients under increasing relative humidity.

Concerning heat transfer, transient thermal transmittance values for north-facing façades in Lisbon met the recommended maximum of 0.5 W/(m²·°C) throughout the year. The south façade did not meet this requirement during the summer months but generally remained below 0.6 W/(m²·°C). In Porto Alegre, the same system met the recommended value for its bioclimatic zone of 2.7 W/(m²·°C) and, for the north façade, it remained below 0.50 W/(m²·°C) throughout the year. The differences between maximum surface thermal transmittance requirements for vertical envelope zones in Porto Alegre and Lisbon are evident.

The use of cork-based thermal mortars, a by-product of the cork industry, yielded good performance regarding local hygrothermal loads and thermal transmittance. However, future work should carefully consider external finishing systems in terms of moisture transmission and further enhance thermal characterization of mortars through effusivity, diffusivity, and variable-humidity conductivity measurements. Additionally, interior climate monitoring should be conducted in typical buildings to validate the conclusions. The validation of external surface condensation results through sensing is recommended. Finally, additional simulations should be carried out assuming the air cavity is ventilated, comparing the final performance of thermal façades with those coated with conventional renders, one-leaf walls, ETICS with panels, and exposing the assembly to more demanding climates. The investigation and practical implementation of this type of solution can serve as a strategy toward more sustainable construction.

# References

ALMEIDA, L. *et al*. 20th Century mortars: physical and mechanical properties from awarded buildings in Lisbon (Portugal): studies towards their conservation and repair. **Buildings**, v. 13, n. 10, 2468, 2023.

AMERICAN SOCIETY FOR TESTING AND MATERIALS. **D7984**: standard test method for measurement of thermal effusivity of fabrics using a modified transient plane source (MTPS) instrument. West Conshohocken, 2021.

ASSOCIAÇÃO BRASILEIRA DE NORMAS TÉCNICAS. **NBR 15220-3**: desempenho térmico de edificações: parte 3: zoneamento bioclimático por desempenho. Rio de Janeiro, 2024.

ASSOCIAÇÃO BRASILEIRA DE NORMAS TÉCNICAS. **NBR 15575-4**: edificações habitacionais: desempenho: parte 4: requisitos para os sistemas de vedações verticais internas e externas: SVVIE. Rio de Janeiro, 2021.

BALTAZAR, L. G.; MORAIS, A. Assessment of the type of paint on performance of rendering mortars. **Coatings**, v. 4, p. 454-468, 2023.

BARAN, I. *et al*. Interstitial condensation risk at thermal rehabilitated buildings. **IOP Conference Series: Materials Science and Engineering**, v. 151, 012084, 2016.

BARREIRA, E.; FREITAS, V. P. de. External thermal insulation composite systems: critical parameters for surface hygrothermal behaviour. **Advances in Materials Science and Engineering**, v. 2014, 650752, 2014.

BEBER, L. A. *et al.* Hydrothermal behavior of hollow ceramic bricks from Southern Brazil brickyard. **Ambiente Construído**, Porto Alegre, v. 24, e138174, jan./dez. 2024.

BECK, H. E. *et al*. Present and future Köppen-Geiger climate classification maps at 1-km resolution. **Scientific Data**, v. 5, 180214, 2018.

BERSCH, J. D. *et al*. Effect of different types of paint on the hygrothermal behavior of facade-rendering mortars in Brazil. **Journal of Architectural Engineering**, v. 30, n. 2, 2024.

BORGES, A.; FLORES-COLEN, I.; BRITO, J. de. Physical and mechanical performance of cement-based renders with different contents of fly ash, expanded cork granules and expanded clay. **Construction and Building Materials**, v. 191, p. 535-543, 2018.

BRÁS, A.; LEAL, M.; FARIA, P. Cement-cork mortars for thermal bridges correction: comparison with cement-EPS mortars performance. **Construction and Building Materials**, v. 49, p. 315-327, 2013.

BULIGON, L. B. *et al.* Hygrothermal performance of masonry walls in residential building in a humid subtropical climate. **PARC Pesquisa em Arquitetura e Construção**, v. 13, 2022.

CHE, X.; ZHU, B.; WANG, P. Assessing global energy poverty: an integrated approach. **Energy Policy**, v. 149, 112099, 2021.

CORRÊA, M. R. S. The evolution of the design and construction of masonry buildings in Brazil. **Gestão & Tecnologia de Projetos**, v. 7, n. 2, 2012.

EUROPEAN COMMISSION. **A renovation wave for Europe**: greening our buildings, creating jobs, improving lives. Brussels, 2020.

EUROPEAN COMMITTEE FOR STANDARDIZATION. **EN 1015-10**: methods of test for mortar for masonry: part 10: determination of dry bulk density of hardened mortar. Brussels, 1999.

EUROPEAN COMMITTEE FOR STANDARDIZATION. **EN 1015-18**: methods of test for mortar for masonry: part 18: determination of water absorption coefficient due to capillary action of hardened mortar. Brussels, 2002.

EUROPEAN COMMITTEE FOR STANDARDIZATION. **EN 1015-3**: methods of test for mortar for masonry: part 3: determination of consistence of fresh mortar (by Flow Table). Brussels, 1999.

EUROPEAN COMMITTEE FOR STANDARDIZATION. **EN 998-1**: specification for mortar for masonry: part 1: rendering and plastering mortar. Brussels, 2010.

EUROPEAN COMMITTEE FOR STANDARDIZATION. **EN ISO 12572**: building materials: determination of water vapor transmission properties. Brussels, 2016.

EUROPEAN COMMITTEE FOR STANDARDIZATION. **EN 15026**: hygrothermal performance of building components and building elements: assessment of moisture transfer by numerical simulation. Brussels, 2023.

EVRARD, A. *et al.* Influence of liquid absorption coefficient on hygrothermal behaviour of an existing brick wall with Lime–Hemp plaster. **Building and Environment**, v. 79, p. 90-100, 2014.

FANG, A.; CHEN, Y.; WU, L. Transient simulation of coupled heat and moisture transfer through multi-layer walls exposed to future climate in the hot and humid southern China area. **Sustainable Cities and Society**, v. 52, 101812, 2020.

FINO, R.; TADEU, A.; SIMÕES, N. Influence of a period of wet weather on the heat transfer across a wall covered with uncoated medium density expanded cork. **Energy and Buildings**, v. 165, p. 118-131, 2018.

FLOOD, C.; SCOTT, L.; GLEESON, W. Application of transient hygrothermal modelling to assess thermal transmittance: a case study in Dublin, Ireland. In: CIB WORLD BUILDING CONGRESS, Tampere, 2016. **Proceedings […]** Tampere: CIB, 2016.

FRAUNHOFER INSTITUTE FOR BUILDING PHYSICS. **WUFI® Pro 6 Manual**. Valley: IBP, 2019.

GAGLIANO, A.; ANELI, S. Analysis of the energy performance of an Opaque Ventilated Façade under winter and summer weather conditions. **Solar Energy**, v. 205, p. 531-544, 2020.

GASPAR, P.; BRITO, J. de. Mapping defect sensitivity in external mortar renders. **Construction and Building Materials**, v. 19, n. 8, p. 571-578, 2005.

GOMES, M. G. *et al.* The influence of moisture content on the thermal conductivity of external thermal mortars. **Construction and Building Materials**, v. 135, p. 279-286, 2017.

GUIZZARDI, M. Hygrothermal performance assessment of novel interior insulation solutions. Zürich, 2014. Thesis – ETH Zürich, 2014.

HENS, H. S. L. C. The vapor diffusion resistance and air permeance of masonry and roofing systems. **Building and Environment**, v. 41, n. 6, p. 745-755, 2006.

INGEBRETSEN, S. B. *et al.* Microclimate and mould growth potential of air cavities in ventilated wooden façade and roof systems: case studies from Norway. **Buildings**, v. 12, n. 1, 1739, 2022.

INSTITUTO NACIONAL DE ESTATÍSTICA; LABORATÓRIO NACIONAL DE ENGENHARIA CIVIL. Edifícios. In: INSTITUTO NACIONAL DE ESTATÍSTICA; LABORATÓRIO NACIONAL DE ENGENHARIA CIVIL. **O Parque habitacional e a sua reabilitação**: análise e evolução 2001-2011. Lisboa: INE, 2013.

INSTITUTO NACIONAL DE METEOROLOGIA. **Arquivos climáticos INMET 2018**. Florianópolis: labEEE, 2018. Disponível em: https://labeee.ufsc.br/pt-br/downloads/arquivos-climaticos/inmet2018. Acesso em: 16 jul. 2020.

INSTITUTO PORTUGUÊS DA QUALIDADE. **NP EN 1936**: métodos de ensaio para pedra natural: determinação das massas volúmicas real e aparente e das porosidades total e aberta. Caparica, 2008.

INSTITUTO PORTUGUÊS DA QUALIDADE. **NP EN 196-1**: métodos de ensaio de cimentos: parte 1: determinação das resistências mecânicas. Caparica, 2006.

INTERNATIONAL ORGANIZATION FOR STANDARDIZATION. **ISO 12571**: hygrothermal performance of building materials and products: determination of hygroscopic sorption properties. Genebra, 2013.

INTERNATIONAL ORGANIZATION FOR STANDARDIZATION. **ISO 12572**: hygrothermal performance of building materials and products: determination of water vapour transmission properties: cup method. Genebra, 2016.

INTERNATIONAL ORGANIZATION FOR STANDARDIZATION. **ISO 13786**: thermal performance of building components: dynamic thermal characteristics: calculation methods. Genebra, 2015.

INTERNATIONAL ORGANIZATION FOR STANDARDIZATION. **ISO 7345**: thermal performance of buildings and building components: physical quantities and definitions. Genebra, 2017.

KAROGLOU, M. *et al.* Effect of coatings on moisture and salt transfer phenomena of plasters. **Construction and Building Materials**, v. 48, p. 35-44, 2013.

KLEBER, D. H. **Análise do desempenho de sistemas de vedação vertical externo com diferentes tipos de argamassa, através de simulação higrotérmica para a cidade de Porto Alegre**. Porto Alegre, 2018. Trabalho de Conclusão de Curso (Engenharia Civil) – Universidade Federal do Rio Grande do Sul, Porto Alegre, 2018.

KRAUSE, P.; POKORSKA-SILVA, I.; KOSOBUCKI, Ł. Determining moisture condition of External Thermal Insulation Composite System (ETICS) of an Existing Building. **Materials**, v. 18, n. 3, 614, 2025.

KÜNZEL, H. M. Factors determining surface moisture on external walls. In: BUILDINGS CONFERENCE, 10., Atlanta, 2007. **Proceedings […]** Atlanta: ASHRAE, 2007.

KÜNZEL, H. M. **Simultaneous heat and moisture transport in building components**: one- and two-dimensional calculation using simple parameters. Stuttgart, 1995. Thesis – Fraunhofer IRB Verlag, Stuttgart, 1995.

LIU, L. *et al.* Description of phase change materials (PCMs) used in buildings under various climates: a review. **Journal of Energy Storage**, v. 56, n. A, 105760, 2022.

MAIA, J.; RAMOS, N. M. M.; VEIGA, R. Evaluation of the hygrothermal properties of thermal rendering systems. **Building and Environment**, v. 144, p. 437-449, 2018.

MALANHO, S.; VEIGA, R.; FARINHA, C. B. Global performance of sustainable thermal insulating systems with cork for building facades. **Buildings**, v. 11, n. 3, 83, 2021.

MARTIN-GARÍN, A. *et al.* Improving energy performance of historic buildings through hygrothermal assessment of the envelope. **Buildings**, v. 11, n. 8, 410, 2021.

MARTÍNEZ-SALA, A. S. *et al.* IoT sensor system for monitoring thermal inertia and climate efficiency in a residential house with double leaf opaque façade. **Journal of Building Engineering**, v. 111, 113220, 2025.

PARRACHA, J. L. *et al.* Effects of hygrothermal and natural aging on the durability of multilayer insulation systems incorporating thermal mortars with EPS and aerogel. **Cement and Concrete Composites**, v. 148, 105843, 2024a.

PARRACHA, J. L. *et al.* Hygrothermal behaviour of External Thermal Insulation Composite Systems (ETICS) to withstand biological colonisation. **Journal of Building Engineering**, v. 86, 108932, 2024b.

PARRACHA, J. L. *et al.* Performance of lightweight thermal insulating mortars applied on brick substrate specimens and prototype wall. **Construction and Building Materials**, v. 364, 129954, 2023.

PEDROSO, M. *et al.* Thermophysical parameters and hygrothermal simulation of aerogel-based fibre-enhanced thermal insulating renders applied on exterior walls. **Energies**, v. 16, 3048, 2023.

PENGFEI, Z.; CHI, Z.; WANG, J. Influence of the Passive Design of a Building Facade on the Indoor Thermal Comfort of Residential Buildings. **E3S Web of Conferences**, v. 237, 03006, 2021.

PINCHARD, L. *et al.* Weather ageing effects on the long-term thermal conductivity and biological colonisation of thermal insulating mortars with EPS, cork and aerogel. **Energy and Buildings**, v. 317, 114403, 2024.

POSANI, M.; VEIGA, R.; FREITAS, V. P. de. Thermal renders for traditional and historic masonry walls: comparative study and recommendations for hygric compatibility. **Building and Environment**, v. 228, 109737, 2023.

POSANI, M.; VEIGA, R.; FREITAS, V. P. de. Thermal mortar-based insulation solutions for historic walls: An extensive hygrothermal characterization of materials and systems. Construction and Building Materials, v. 315, 125640, 2022.

RAMOS, N. M. M. *et al.* Probabilistic risk assessment methodology of exterior surfaces defacement caused by algae growth. **Journal of Construction Engineering and Management**, v. 140, p. 050140121-05014017, 2014.

RANESI, A. *et al.* A discussion on winter indoor hygrothermal conditions and hygroscopic behaviour of plasters in southern Europe. **Infrastructures**, v. 7, n. 3, 38, 2022.

REPÚBLICA PORTUGUESA. Portaria Nº 138-I/2021, de 1º de Julho. Ambiente e Ação Climática e Infraestruturas e Habitação. **Diário da República**, 1ª série, p. 128(12), 1 jul. 2021.

REPÚBLICA PORTUGUESA. Portaria Nº 297/2019 de 9 de Setembro. Ambiente e Transição Energética. **Diário da República**, 1ª série, p. 198, 9 set. 2019.

RODRIGUES, E. *et al.* Thermal transmittance effect on energy consumption of Mediterranean buildings with different thermal mass. **Applied Energy**, v. 252, 113437, 2019.

RODRIGUES, E.; PARENTE, J.; FERNANDES, M. S. Building for tomorrow: analyzing ideal thermal transmittances in the face of climate change in Brazil. **Applied Energy**, v. 355, 122360, 2024.

ŠADAUSKIENĖ, J. *et al.* The impact of the exterior painted thin-layer render's water vapour and liquid water permeability on the moisture state of the wall insulating system. **Construction and Building Materials**, v. 23, n. 8, p. 2788-2794, 2009.

SATO, N. M. N. *et al.* Influence of thermal properties of materials in condensation and microorganism growth on building facades. In: DBMC INTERNATIONAL CONFERENCE ON DURABILITY OF BUILDING MATERIALS AND COMPONENTS, 11., Instambul, 2008. **Proceedings […]** Instambul: CIB, 2008.

SOUSA, H. Portuguese masonry building enclosures: practices and problems. In: COMMISSION MEETING, 37., Penn State, 2000. **Proceedings […]** Penn State: CIB, 2000.

SQUADRONI, F. *et al.* Analysis of condensation and ventilation phenomena for double skin façade units. **Journal of Building Physics**, v. 46, n. 2, p. 211-244, 2022.

TENI, M.; ČULO, K.; KRSTIĆ, H. Renovation of public buildings towards nZEB: a case study of a nursing home. **Buildings**, v. 9, n. 7, 153, 2019.

TRONCHIN, L.; FABBRI, K.; TOMMASINO, M. C. A comparison of thermal insulation with interstitial condensation in different climate contexts in existing buildings in Europe. **Energies**, v. 16, n. 4, 1979, 2023.

UNITED NATIONS ENVIRONMENT PROGRAMME. **2021 Global status report for buildings and construction**: towards a zero emission, efficient and resilient buildings and construction sector. Nairobi: UNEP, [2021].

UNITED NATIONS GROUP OF EXPERTS ON GEOGRAPHICAL NAMES. **City details**. New York, 2025.

VANDEMEULEBROUCKE, I. *et al.* Degradation of brick masonry walls in Europe and the Mediterranean: Advantages of a response-based analysis to study climate change. **Building and Environment**, v. 230, 109963, 2023.

VERDUM, G. *et al.* Mortar coating degradation in historical buildings facades from Rio Grande do Sul, Brazil. **Construction and Building Materials**, v. 310, 125221, 2021.

VERMA, S. B. K. *et al.* Hygrothermal dynamics for developing energy-efficient buildings: Building materials and ventilation system considerations. **Energy and Buildings**, v. 260, 111932, 2022.

**Declaration of Generative AI and AI-Assisted Technologies in the Writing Process**
During the preparation of this work the authors used ChatGPT in order to to check grammar issues and to improve readability. After using this tool/service, the authors reviewed and edited the content as needed and take(s) full responsibility for the content of the publication.

**Financial Support**
This research was funded by the Fundação para a Ciência e a Tecnologia, I.P. (FCT, https://ror.org/00snfqn58) under Grant UID/6438/2025 of the research unit CERIS, the grant number 2023.05316.BD (DOI: https://doi.org/10.54499/2023.05316.BD) of Author 1, and the ReCoveRing project. The authors acknowledge the support from Instituto Superior Técnico, Programa de Pós-Graduação em Engenharia Civil: Construção e Infraestrutura (PPGCI) Universidade Federal do Rio Grande do Sul (UFRGS), Conselho Nacional de Desenvolvimento Tecnológico (CNPq), and Fundação Coordenação de Aperfeiçoamento de Pessoal de Nível Superior (CAPES).

**Data Availability Statement**
Research data is available in the body of the article.

**Conflict of Interest**
Não há conflito de interesse.

**Authors' Contribution**
**Jéssica D. Bersch:** Conceptualization, Formal analysis, Investigation, Methodology, Software, Visualization, Writing – original draft, Writing – review & editing. **Angela B. Masuero**: Conceptualization, Supervision, Writing – review & editing. **Denise C. Dal Molin**: Conceptualization, Supervision, Writing – review & editing. **Inês Flores-Colen**: Conceptualization, Methodology, Funding acquisition, Project administration, Supervision, Writing – review & editing.

Editor-in-chief: **Enedir Ghisi**
Guest editor: **Juliana Machado Casali Peruch**

***Ambiente Construído***
Revista da Associação Nacional de Tecnologia do Ambiente Construído
Av. Osvaldo Aranha, 99 - 3º andar, Centro
Porto Alegre – RS - Brasil
CEP 90035-190
Telefone: +55 (51) 3308-4084
www.seer.ufrgs.br/ambienteconstruido
www.scielo.br/ac
E-mail: ambienteconstruido@ufrgs.br